

# The localization transition at finite temperatures: electric and thermal transport

Article for: "50 Years of Anderson Localization"

Yoseph Imry<sup>1,\*</sup> and Ariel Amir<sup>1</sup>

<sup>1</sup>*Department of Condensed Matter Physics, Weizmann Institute of Science, Rehovot 76100, Israel*

(Dated: October 24, 2018)

The Anderson localization transition is considered at finite temperatures. This includes the electrical conductivity as well as the electronic thermal conductivity and the thermoelectric coefficients. An interesting critical behavior of the latter is found. A method for characterizing the conductivity critical exponent, an important signature of the transition, using the conductivity and thermopower measurements, is outlined.

PACS numbers: 72.15.Cz, 72.15.Rn, 72.20.Pa

## I. INTRODUCTION

Anderson localization<sup>1,2</sup> is a remarkable, and very early, example of a quantum phase transition (QPT), where the nature of a system at  $T = 0$  changes abruptly and nonanalytically at a point, as a function of a control parameter. Here it implies that the relevant quantum states of the system acquire an exponential decay at large distances (similar to, but much more complex than, the formation of a bound state). In the original paper this phenomenon was discovered via a change in the convergence properties of the "locator" expansion. In the disordered tight-binding model, with short-range hopping, this is the expansion about the bound atomic, or Wannier-type orbitals. As long as the expansion converges, the relevant eigenstates are localized; its divergence signifies the transition to "extended", delocalized states. This was reviewed, hopefully pedagogically, in Ref. [3]. Later, Mott introduced the very useful picture of the "mobility edge" within the band of allowed energies, separating localized from extended states.<sup>2</sup> In the lower part of the band, the states below the "lower mobility edge" are localized, while those above it are extended. When the disorder and/or the position of the Fermi level,  $E_F$ , are changed, a point where they cross each other is where the states at  $E_F$  change nature from extended to localized, and this is a simple and instructive model for a metal-insulator transition at vanishing temperature  $T$ .

The analysis of the above localization transition centers on the behavior of  $\sigma_0(E)$ , the conductivity at energy  $E$ , which would be the  $T = 0$  conductivity of the sample with  $E_F = E$ .  $\sigma_0(E)$  vanishes for  $E$  below the lower mobility edge  $E_m$  and goes to zero when  $E$  approaches  $E_m$  from above<sup>4</sup>

$$\sigma_0(E) = A(E - E_m)^x. \quad (1)$$

The characteristic exponent for this,  $x$ , is an important parameter of the theory. It is expected to be universal for a large class of noninteracting models, but its value is not really known, in spite of the several analytical, numerical and experimental methods used to attempt its evaluation.

The electron-electron interaction is certainly relevant

near this transition, which may bring it to a different universality class. This is a difficult problem. The benchmark treatment is the one by Finkel'stein.<sup>5</sup> Since it is likely that the situation in at least most experimental systems is within this class, it would appear impossible to determine the value of  $x$  for the pure Anderson transition (without interactions).<sup>6</sup>

In this paper we still analyze the thermal and thermoelectric transport for a general model with  $\sigma_0(E)$  behaving as in Eq. (1). This is certainly valid for noninteracting electrons and should be valid also including the interactions, as long as some kind of Landau Fermi-liquid quasiparticles exist. In that case  $\sigma_0(E)$  for quasiparticles is definable and thermal averaging with Fermi statistics holds. Even then, however, various parameter renormalizations and interaction corrections<sup>7</sup> should come in. The effect of the interactions on the thermopower for a small system in the Coulomb blockade picture was considered in Ref. [8], and correlations were included in Ref. [9]. Even in the latter case, the simple Cutler-Mott<sup>10</sup> formula (Eq. 22, derived in section III) was found to work surprisingly well.

It should be mentioned that the sharp and asymmetric energy-dependence of  $\sigma_0(E)$  near the mobility edge<sup>10,11</sup> should and does<sup>10,12,13</sup> lead to rather large values of the thermopower. Exceptions will be mentioned and briefly discussed later. Large thermopowers are important for energy conversion and refrigeration applications<sup>14</sup> and this clearly deserves further studies.

A serious limitation on the considerations presented here is that the temperature should be low enough so that all the inelastic scattering (electron-phonon, electron-electron, etc.) is negligible. For simplicity we consider here *only* longitudinal transport (currents parallel to the driving fields). Thus, no Hall or Nernst-Ettinghausen effect! We also do not consider the thermoelectric transport in the hopping regime. It might be relevant even in the metallic regime (chemical potential  $\mu > E_m$ ), once  $k_B T \gtrsim \mu - E_m$ . This may well place limitations on the high temperature analysis we make in the following.

In section II we review the basic concepts behind the scaling theory<sup>4</sup> for the transition, and reiterate the critical behavior of the conductivity as in Eq. (1), obtaining

also its temperature dependence. In section III we derive all results for the thermal and thermoelectric transport and analyze the scaling critical behavior of the latter as function of temperature and distance from the transition. A brief comparison with experiment is done in section IV and concluding remarks are given in section V. In the appendix we present a proof that the heat carried by a quasiparticle is equal to its energy measured from the chemical potential,  $\mu$ , hoping that this also clarifies the physics of this result. This derivation is valid for Bose quasiparticles (phonons, photons, magnons, excitons, plasmons, etc.) as well.

## II. THE ZERO AND FINITE TEMPERATURE MACROSCOPIC CONDUCTIVITY AROUND THE ANDERSON LOCALIZATION TRANSITION

### A. The Thouless picture within the tunnel-junction model

We start this section by briefly reviewing the tunnel-junction picture of conduction<sup>15,16</sup> at  $T = 0$ , which is a useful way to understand the important Thouless<sup>17</sup> picture for such transport. Consider first two pieces (later referred to as “blocks”) of a conducting material with a linear size  $L$ , connected through a layer of insulator (usually an oxide) which is thin enough to allow for electron tunneling. The interfaces are assumed rough, so there is no conservation of the transverse momentum: each state on the left interacts with each state on the right with a matrix element  $t$  with a roughly uniform absolute value. The lifetime  $\tau_L$  for an electron on one such block for a transition to the other one is given by the Fermi golden rule (at least when tunneling is a weak perturbation):

$$\tau_L^{-1} = \frac{2\pi}{\hbar} \overline{|t|^2} N_r(E_F), \quad (2)$$

where  $\overline{|t|^2}$  is the average of the tunneling matrix element squared and  $N_r(E_F)$  is the density of states on the final (right-hand) side. Taking the density of states (DOS) in the initial side to be  $N_\ell(E_F)$ , we find that when a voltage  $V$  is applied,  $eVN_\ell(E_F)$  states are available, each decaying to the right with a time constant  $\tau_L$ , so that the current is

$$I = e^2 N_\ell(E_F) \tau_L^{-1} V, \quad (3)$$

and the conductance is

$$G = e^2 N_\ell(E_F) / \tau_L = \frac{2\pi e^2}{\hbar} \overline{|t|^2} N_\ell(E_F) N_r(E_F), \quad (4)$$

which is an extremely useful result. This equality is well-known in the tunnel junction theory.<sup>15,16</sup> Clearly,  $G$  is symmetric upon exchanging  $l$  and  $r$ , as it should.<sup>18</sup> Note that Eqs. (2) and (4) are valid in any number of dimensions. An important remark is that Eq. (2) necessitates a continuum of final states, while the final (RHS) block

is finite and has a discrete spectrum. One must make the assumption that the interaction of that system with the outside world leads to a level broadening larger than, or on the same order of, the level spacing.<sup>19–21</sup> This is the case in most mesoscopic systems. One then naively assumes that this condition converts the spectrum to an effectively continuous one (the situation may actually be more subtle).<sup>22</sup> Otherwise, when levels really become discrete, one gets into the *really microscopic (molecular) level*.

The result of Eq. (4) is very general. Let us use it for the following scaling picture<sup>17</sup>: Divide a large sample to (hyper) cubes or “blocks” of side  $L$ . We consider the case  $L \gg \ell, a$ ;  $\ell$  being the elastic mean free path and  $a$  the microscopic length. The typical level separation for a block at the relevant energy (say, the Fermi level),  $d_L$ , is given by the inverse of the density of states (per unit energy) for size  $L$ ,  $N_L(E_F)$ . Defining an energy associated with the transfer of electrons between two such adjacent systems by  $V_L \equiv \pi\hbar/\tau_L$  ( $\tau_L$  is the lifetime of an electron on one side against transition to the other side) the dimensionless interblock conductance  $g_L \equiv G_L/(e^2/\pi\hbar)$  is:

$$g_L = V_L/d_L \quad (5)$$

i.e.  $g_L$  is the (dimensionless) ratio of the only two relevant energies in the problem. The way Thouless argued for this relation is by noting that the electron’s diffusion on the scale  $L$  is a random walk with a step  $L$  and characteristic time  $\tau_L$ , thus

$$D_L \sim L^2/\tau_L$$

Note that as long as the classical diffusion picture holds,  $D_L$  is independent of  $L$  and  $\tau_L = L^2/D$ , which is the diffusion time across the block. It will turn out that the localization or quantum effects, when applicable, cause  $D_L$  to decrease with  $L$ . For metals, the conductivity,  $\sigma_L$ , on the scale of the block size  $L$ , is given by the Einstein relation  $\sigma = D_L e^2 dn/d\mu$  (where  $\mu$  is the chemical potential and  $dn/d\mu$  is the density of states per unit volume), and the conductance in  $d$  dimensions is given by:

$$G_L = \sigma_L L^{d-2}. \quad (6)$$

Putting these relations together and remembering that  $N_L(E_F) \sim L^d dn/d\mu$ , yields Eq. (5).

To get some physical feeling for the energy  $h/\tau_L$  we note again that, at least for the weak coupling case, the Fermi golden rule yields Eq. (2) or:

$$V_L = 2\pi^2 \overline{|t|^2} / d_r. \quad (7)$$

Thus,  $V_L$  is defined in terms of the interblock matrix elements. Clearly, when the blocks are of the same size, Eq. (7) is also related to the order of magnitude of the second order perturbation theory shift of the levels in one block by the interaction with the other. For a given block this is similar to a surface effect – the shift in the

block levels due to changes in the boundary conditions on the surface of the block. Indeed, Thouless has given appealing physical arguments for the equivalence of  $V_L$  with the sensitivity of the block levels to boundary conditions. This should be valid for  $L$  much larger than  $\ell$  and all other microscopic lengths.

Since in this scaling picture the separations among the blocks are fictitious for a homogeneous system, it is clear that the interblock conductance is just the conductance of a piece whose size is of the order of  $L$ , i.e., this is the same order of magnitude as the conductance of the block itself.

The latter can also be calculated using the Kubo linear response expression. It has to be emphasized that the Kubo formulation also applies strictly only for an infinite system whose spectrum is continuous. For a finite system, it is argued again that a very small coupling of the electronic system to some large bath (e.g. the phonons, or to a large piece of conducting material) is needed to broaden the discrete levels into an effective continuum. Edwards and Thouless,<sup>23</sup> using the Kubo-Greenwood formulation, made the previously discussed relationship of  $V_L$  with the sensitivity to boundary conditions very precise.

The above picture is at the basis of the finite-size scaling<sup>4,24</sup> theory of localization. It can also be used for numerical calculations of  $g(L)$ , which is a most relevant physical parameter of the problem, for non-interacting electrons, as we shall see. Alternatively, Eq. (7) as well as generalizations thereof can and have been used for numerical computations. Powerful numerical methods exist to this end.<sup>25</sup>

It is important to emphasize that  $g_L \gg 1$  means that states in neighboring blocks are tightly coupled while  $g_L \ll 1$  means that the states are essentially single-block ones.  $g_L$  is therefore a good general dimensionless measure of the strength of the coupling between two quantum systems. Thus, if  $g_L \gg 1$  for small  $L$  and  $g_L \rightarrow 0$  for  $L \rightarrow \infty$ , then the range of scales  $L$  where  $g_L \sim 1$  gives the order of magnitude of the localization length,  $\xi$ .

Although the above analysis was done specifically for non-interacting electrons, it is of greater generality.  $g_L$  (with obvious factors) may play the role of a conductance also when a more general entity (e.g. an electron pair) is transferred between the two blocks. The real limitations for the validity of this picture seem to be the validity of the Fermi-liquid picture and that no inelastic effects (e.g. with phonons or electron-hole pairs) occur.

The analysis by Thouless<sup>17</sup> of the consequences of Eq. (5) for a long thin wire has led to extremely important results. First, it showed that 1D localization should manifest itself not only in “mathematically 1D” systems but also in the conduction in realistic, finite cross-section, thin wires, demonstrating also the usefulness of the block-scaling point of view. Second, the understanding of the effects of finite temperatures (as well as other experimental parameters) on the relevant scale of the conduction, clarifies the relationships between  $g(L)$  and experiment

in any dimension. Third, defining and understanding the conductance  $g(L)$  introduces the basis for the scaling theory of the Anderson localization transition.<sup>4</sup> Here, we use the results for the (macroscopic)  $T = 0$  conductivity around the localization transition to get the finite temperature conductivity there.

## B. The critical behavior of the $T = 0$ conductivity

Near, say, the lower mobility edge,  $E_m$ , the conductivity  $\sigma_0(E)$  vanishes for  $E < E_m$  and approaches zero for  $E \rightarrow E_m$  from above, in the manner:

$$\sigma_0(E) = A(E - E_m)^x, \quad (8)$$

$A$  being a constant and  $x$  the conductivity critical exponent for localization, which has so far eluded a precise determination either theoretically or experimentally. Within the scaling theory,<sup>4</sup>  $x$  is equal to the critical exponent of the characteristic length ( $\xi$ ), because

$$\sigma \sim \frac{e^2}{\pi\hbar\xi}. \quad (9)$$

In that case, an appealing intuitive argument by Mott<sup>27</sup> and Harris<sup>26</sup> places a lower bound on  $x$ :

$$x \geq 2/d. \quad (10)$$

In fact, Eq. (9) may be expected to hold on dimensional grounds for any theory which does not generate another critical quantity with the dimension of length. This should be the case for models which effectively do not have electron-electron interactions. With electron-electron interactions, for example, we believe that the critical exponent for the characteristic length should satisfy an inequality such as Eq. (10).<sup>28</sup> However, this may no longer be true for the conductivity exponent.

## C. The conductivity at finite temperatures

In Eqs. (3) and (4) we calculated, at  $T = 0$ , the current in an infinitesimal (linear response) energy strip of width  $eV$  around the Fermi energy. Generalizing this to an arbitrary energy at finite temperature, we find that the current due to a strip  $dE$  at energy  $E$  is

$$I(E)dE = eN_\ell(E_F)\tau_L^{-1}(E)[f_l(E) - f_r(E)]dE, \quad (11)$$

$f_l(E)$  ( $f_r(E)$ ) being the Fermi function at energy  $E$  at the left (right). The total current is obtained by integrating Eq. (11) over energy. For linear response  $f_l(E) - f_r(E) = eV[-\frac{\partial f}{\partial E}]$ . This gives

$$\sigma(T) = \int_{-\infty}^{\infty} dE \sigma_0(E) \left[-\frac{\partial f}{\partial E}\right], \quad (12)$$

where  $\sigma_0(E) \equiv (e^2/\pi\hbar)\frac{V_L(E)}{d_L(E)}L^{(2-d)}$  is the conductivity (using Eqs. 5 and 6) at energy  $E$ , which would be the  $T = 0$  conductivity of the sample with  $E_F = E$ .

#### D. Analysis of $\sigma(T, \mu - E_m)$

From now on we assume Eq. (8) to hold. Measuring all energies from the chemical potential  $\mu$  and scaling them with  $T$ , we rewrite Eq. (12) in the manner (we shall employ units in which the Boltzmann constant,  $k_B$  is unity, and insert it in the final results)

$$\sigma(T, \mu - E_m) = AT^x \Sigma([\mu - E_m]/T), \quad (13)$$

where the function  $\Sigma(z)$  is given by:

$$\Sigma(z) \equiv \int_{-z}^{\infty} dy (y+z)^x \left[ -\frac{\partial [1 + \exp(y)]^{-1}}{\partial y} \right]. \quad (14)$$

Fig. 1 shows a numerical evaluation of this integral.

Let us consider the low and high temperature limits of this expression, that will also be useful later for the analysis of the thermopower.

At low temperatures, we can use the Sommerfeld expansion, to obtain:

$$\sigma_{low}(T)/A = (\mu - E_m)^x + \frac{\pi^2}{6} T^2 x(x-1) (\mu - E_m)^{x-2}. \quad (15)$$

Notice that  $\frac{\partial \sigma}{\partial T}$  is negative for  $x < 1$ : this comes about since in this case the function  $\sigma(E)$  is concave.

At high temperatures, one can set  $E_m = 0$ , since the contribution to the integrals comes from energies smaller or of the order of the temperature, and  $T \gg \mu - E_m$ . Therefore we have to evaluate:

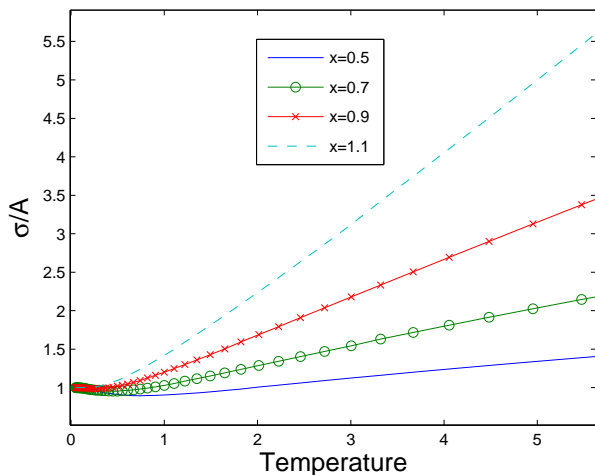


FIG. 1: The integral of Eq. (14) was evaluated numerically, for different values of the exponent  $x$ , for  $\mu - E_m = 1$ . Shown is the dependence of the conductivity, measured in units of  $A$  (see Eq. (8)) as a function of temperature (the energy scale is set by  $\mu - E_m$ ). At low temperatures, the conductivity saturates to a value given by Eq. (15), while at high temperatures it scales as  $T^x$ , see Eq. (16). The derivative at low temperatures can be positive or negative, depending on  $x$  (see Eq. (15)).

$$\sigma_{high}(T)/A = \int_0^{\infty} E^x \left( -\frac{\partial f}{\partial E} \right) dE. \quad (16)$$

Thus, at high temperatures  $\sigma_{high}/A \sim T^x$ , with the coefficient given by  $\int_0^{\infty} \frac{q^x}{2 + \cosh(q)} dq$ . In section III C we show that this integral can be connected with the Riemann Zeta function, and its value is given by Eq. (36).

This scaling could be used for a determination of the exponent  $x$ . However a much closer determination of that exponent would follow from the scaling of both the conductivity and the thermal and thermoelectric transport coefficients, which will be studied in the coming sections.

### III. THERMAL AND THERMOELECTRIC TRANSPORT

#### A. General relationships

Consider now the case where both a voltage  $V$  and a temperature difference  $\Delta T$  are applied between the two blocks. We choose for convenience  $k_B \equiv 1$ . Both are small enough for linear response to hold. Here we have to replace the Fermi function difference in Eq. (11) by

$$f_l(E) - f_r(E) = eV \left[ -\frac{\partial f}{\partial E} \right] + \Delta T \left[ -\frac{\partial f}{\partial T} \right].$$

Then generalizing Eq. (12) yields for the electrical current

$$I = \int dE \frac{G(E)}{e} \left\{ \left[ -e \frac{\partial f}{\partial E} \right] V + \left[ -\frac{\partial f}{\partial T} \right] \Delta T \right\}, \quad (17)$$

with  $G$  given in Eq. (6). The first term is the ordinary ohmic current and the second one is the thermoelectric charge current due to the temperature gradient.

Next, we derive the heat current. The heat carried by an electron with energy  $E$  (measured from the chemical potential,  $\mu$ ) is equal to  $E$ . This is shown, for example in Ref. [30] by noting that the heat is the difference between the energy and the free energy. Sivan and Imry<sup>11</sup> verified it in their Landauer-type model by calculating the flux of  $TS$  along the wire connecting the two reservoirs. In the appendix, we obtain the same result in our block model, from the time derivative of the entropy of each block. Thus, we obtain the heat current  $I_Q$ ,

$$I_Q = \int dE E \frac{G(E)}{e^2} \left\{ \left[ -e \frac{\partial f}{\partial E} \right] V + \left[ -\frac{\partial f}{\partial T} \right] \Delta T \right\}. \quad (18)$$

Here the first term is the thermoelectric heat current due to the voltage, while the second one is the main contribution to the usual electronic thermal conductivity  $\kappa$ .

In this model the ratio of *thermal* to electrical conductivities is of the order of  $(k_B/e)^2 T$ . This is because a typical transport electron carries a charge  $e$  and an excitation energy of the order of  $k_B T$  and the driving forces

are the differences in  $eV$  and  $k_B T$ . This ratio is basically the Wiedemann-Franz law.

It is convenient to summarize Eqs. (17) and (18) in matrix notation<sup>29</sup>:

$$\begin{pmatrix} I \\ I_Q \end{pmatrix} = \begin{pmatrix} L_{11} & L_{12} \\ L_{21} & L_{22} \end{pmatrix} \begin{pmatrix} V \\ \Delta T \end{pmatrix}, \quad (19)$$

where the coefficients  $L_{ij}$  can be read off Eqs. (17) and (18). Since  $f$  is a function of  $E/T$ , we see that

$$-\frac{\partial f}{\partial T} = \frac{E}{T} \frac{\partial f}{\partial E} \quad (20)$$

Therefore, the two ‘‘nondiagonal’’ thermoelectric coefficients: the one relating  $I$  to  $\Delta T$ ,  $L_{12}$ , and the one relating  $I_Q$  to  $V$ ,  $L_{21}$ , are equal within a factor  $T$ .

$$L_{12} = L_{21}/T. \quad (21)$$

This is an Onsager<sup>29–32</sup> relationship, which holds very generally for systems obeying time-reversal symmetry (and particle conservation – unitarity). The case where time-reversal symmetry is broken, say by a magnetic field, is briefly discussed in the next subsection.

We conclude this subsection by defining and obtaining an expression for the absolute thermoelectric power (henceforth abbreviated as just ‘‘thermopower’’) of a material. Suppose we apply a temperature difference  $\Delta T$  across a sample which is open circuited and therefore no current can flow parallel to  $\Delta T$ . To achieve that, the sample will develop a (usually small) voltage  $V$ , so that the combined effect of both  $\Delta T$  and  $V$  will be a vanishing current. From Eqs. (17), (19) and (20) we find that the ratio between  $V$  and  $\Delta T$ , which is defined as the thermopower,  $S$ , is given by

$$S \equiv \frac{V}{\Delta T} = -\frac{L_{12}}{L_{11}} = \frac{\int dE E \sigma_0(E) \frac{\partial f}{\partial E}}{eT \int dE \sigma_0(E) \frac{\partial f}{\partial E}}. \quad (22)$$

### B. Onsager relations in a magnetic field

From time-reversal symmetry at  $H = 0$  and unitarity (particle conservation) follows the Onsager relation<sup>29–32</sup> for the  $T = 0$  conductance

$$\sigma(E, H) = \sigma(E, -H). \quad (23)$$

This can be proven for our model from the basic symmetries of the interblock matrix elements. This symmetry obviously follows for the temperature-dependent electrical and thermal conductivities  $\sigma(T)$  and  $\kappa(T)$ .

For the nondiagonal coefficients, the usual Onsager symmetry reads

$$L_{12}(H) = L_{21}(-H)/T. \quad (24)$$

In our case, since the nondiagonal coefficients are expressed as integrals over a symmetric function (Eq. (23)), they also obey

$$L_{ij}(H) = L_{ij}(-H). \quad (25)$$

*i.e.* the nondiagonal coefficients are symmetric in  $H$  as well.

### C. Analysis of the thermopower

Eq. (22) for the thermopower is identical to the one derived in two-terminal linear transport within the Landauer formulation in Ref. [11], which is equal in the appropriate limit to the Cutler-Mott<sup>10,27</sup> expression:

$$S = \frac{\int_{E_m}^{\infty} dE (E - \mu) \sigma_0(E) (-\frac{\partial f}{\partial E})}{e\sigma(T)T}, \quad (26)$$

where  $\mu$  is the chemical potential,  $\sigma_0(E)$  is the conductivity for carriers having energy  $E$  and  $\sigma$  is the total conductivity. The Physics of this formula is clear for the (Onsager-dual) Peltier coefficient: a carrier at energy  $E$  carries an excitation energy (similar to heat, see the appendix) of  $E - \mu$ .

Clearly, electrons and holes contribute to  $S$  with opposite signs.  $S$  will tend to vanish with electron-hole symmetry and will be small, as happens in many metals, especially in ordered ones, when the variation in energy of  $\sigma_0(E)$  around  $\mu$  is weak.

Having a strong energy dependence of  $\sigma_0(E)$ , and being very different above and below  $\mu$  will cause relatively large values of  $S$ . We believe that this is what happens in disordered narrow-gap semiconductors, which feature in many present-day good thermoelectrics. As noted in Refs. [10,11], the Anderson metal-insulator transition (or at least its vicinity) offers an almost ideal situation for large thermopowers. There,  $\sigma_0(E)$  vanishes below the mobility edge  $E_M$  (for electrons) and approaches zero, probably with an infinite slope, above it. Hopping processes in the localized phase are not considered here. A brief analysis in Ref. [11] demonstrated that  $S$  scales with  $z \equiv (\mu - E_M)/T$ :

$$S = Y\left(\frac{\mu - E_M}{T}\right), \quad (27)$$

( $Y$  being a universal scaling function) and assumes the two limits:

$$S \sim (\mu - E_m)^{-1}, \quad \text{for } z \gg 1; \quad (28)$$

and

$$S \sim \text{const} - z, \quad \text{for } z \ll 1. \quad (29)$$

Of course, there is no ‘‘real’’ divergence of  $S$ ,<sup>33</sup> since when  $(\mu - E_m) \rightarrow 0$  (and the slope of  $S(T)$  diverges), it will eventually become smaller than  $T$  and the large-slope linear behavior will saturate as in Eq. (29).

Fig. 2 shows a numerical evaluation of Eq. (26), demonstrating the linear low temperature regime and the saturation at high temperatures. Let us now make a more thorough investigation of the low and high temperature regimes.

For low temperatures, we can use, as before, the Sommerfeld expansion for the nominator and denominator, to obtain:

$$S_{low} \approx \frac{\frac{\pi^2}{3}Tx(\mu - E_m)^{x-1} + O(T^3)}{e[(\mu - E_m)^x + \frac{\pi^2}{6}T^2x(x-1)(\mu - E_m)^{x-2} + O(T^4)]} \quad (30)$$

A more complete expression is give in Eq. (40) below.

Thus, at  $T \ll \mu - E_m$ , the thermopower is linear in temperature:

$$S_{low} \approx \frac{\pi^2 x T}{3e(\mu - E_m)} + O(T^3). \quad (31)$$

Fig. 3 compares this expression with the numerically evaluated slope.

At high temperatures, one can set  $E_m = 0$ , as before. Therefore we have to evaluate:

$$S_{high} = \frac{\int_0^\infty E^{x+1}(-\frac{\partial f}{\partial E})dE}{eT \int_0^\infty E^x(-\frac{\partial f}{\partial E})dE}. \quad (32)$$

We can write  $\int_0^\infty E^\beta(-\frac{\partial f}{\partial E})dE = T^{\beta+2}G(\beta)$ , with the dimensionless function  $G(\beta)$  defined as:

$$G(\beta) = \int_0^\infty \frac{m^\beta}{2 + \cosh(m)} dm. \quad (33)$$

We then have  $S_{high} = \frac{G(x+2)}{eG(x+1)}$ .

In fact, the integral of Eq. (33) can be related to the Riemann Zeta function  $\zeta$ :

$$\zeta(\beta) = \frac{1}{\Gamma(\beta)} \int_0^\infty \frac{m^{\beta-1}}{e^m - 1} dm. \quad (34)$$

Defining  $C = \int_0^\infty \frac{m^{\beta-1}}{e^m - 1} dm$ , we find that:

$$C - G/\beta = \int_0^\infty \frac{2m^{\beta-1}}{e^{2m} - 1} dm = C/2^\beta, \quad (35)$$

therefore:

$$G(\beta) = \beta C(1 - 1/2^{\beta-1}) = \beta \zeta(\beta) \Gamma(\beta) (1 - 1/2^{\beta-1}). \quad (36)$$

This gives an exact formula for the thermopower at high temperatures:

$$S_{high} = (1+x) \frac{\zeta(1+x)(2^x - 1)}{e \zeta(x)(2^x - 2)}. \quad (37)$$

At  $x = 0$ , one obtains  $S = 2 \log(2)$ , while for  $x \gg 1$ , one obtains  $S_{high} \approx 1 + x$ .

Actually, understanding the behavior for large  $x$  is simple: If we were to approximate the derivative of the Fermi-function by  $e^{-E/T}$ , we would have  $G(\beta) = \Gamma(\beta)$ , where  $\Gamma$  stands for the Gamma function. Then, by its properties, we immediately have that  $S_{high} \approx (1+x)/e$ .

It turns out that a good approximation to  $S_{high}(x)$  can be obtained by interpolating the exact  $x = 0$  result and the large  $x$  result, by the form:

$$S_{high} \approx \frac{1}{e} [2 \log(2) + x]. \quad (38)$$

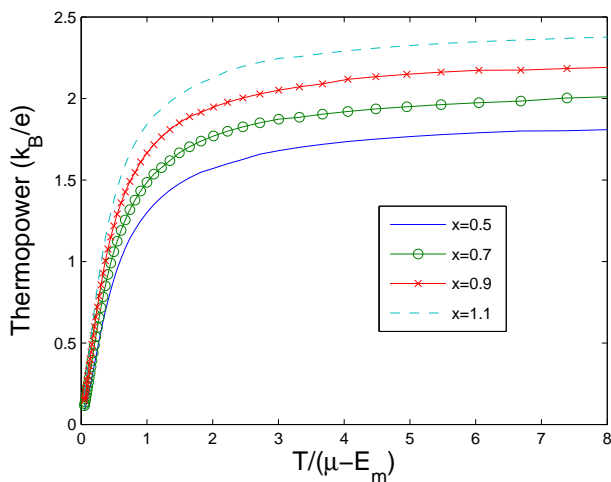


FIG. 2: The integrals of Eq. (26) were evaluated numerically, for different values of the exponent  $x$ . At low temperatures, the thermopower is linear with temperature, while at high temperatures it saturates, to a value which depends on  $x$ .

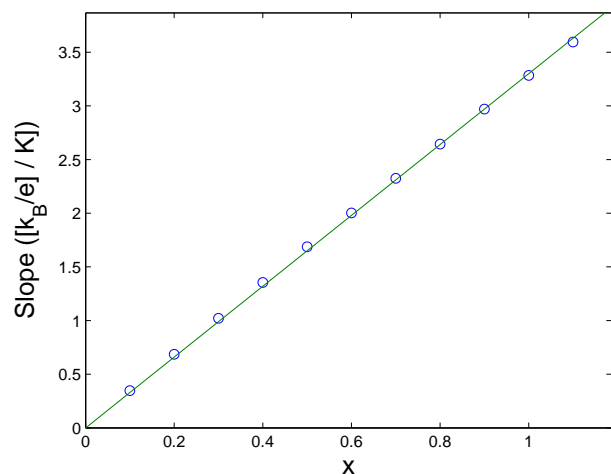


FIG. 3: At low temperatures, the thermopower is described by Eq. (30). The plot shows a comparison between this expression and the evaluation of the slope extracted from the numerics demonstrated in Fig. 2.

Fig. 4 compares the exact saturation values of Eq. (37) with this approximate form. We found that the difference for all values of  $x$  is less than 6 percent, and therefore Eq. (38) provides a practical working formula for the saturation value of the thermopower.

An interesting feature of the crossover from the low to high temperature regime, is the possibility of an inflection point in the thermopower dependence. Similar to the behavior of the conductance, which grew for  $x > 1$  but diminished for  $x < 1$ , here there will be an inflection point for  $x < 1$ . To see this, we have to calculate the next order in the Sommerfeld expansion in the nominator  $Q$  of Eq. (30), to obtain, up to corrections of order  $O(T^5)$ :

$$Q = \frac{\pi^2}{3} T x (\mu - E_m)^{x-1} + \frac{7\pi^4}{90} T^3 x(x-1)(x-2)(\mu - E_m)^{x-3}. \quad (39)$$

This leads to the following low temperature correction of the thermopower:

$$S_{low} \approx \frac{\pi^2 x T}{3e(\mu - E_m)} + \frac{\pi^4}{45} x(x-1)(x-7) \frac{T^3}{e(\mu - E_m)^3} + O(T^5), \quad (40)$$

implying an inflection point for  $x < 1$ .

#### IV. BRIEF DISCUSSION OF EXPERIMENTS

Large thermopowers that are linear in the temperature, at least in the metallic regime, were already found in the pioneering extensive work on Cerium sulfide compounds by Cutler and Leavy,<sup>12</sup> and analyzed by Cutler and Mott.<sup>10</sup> It is interesting to address specifically

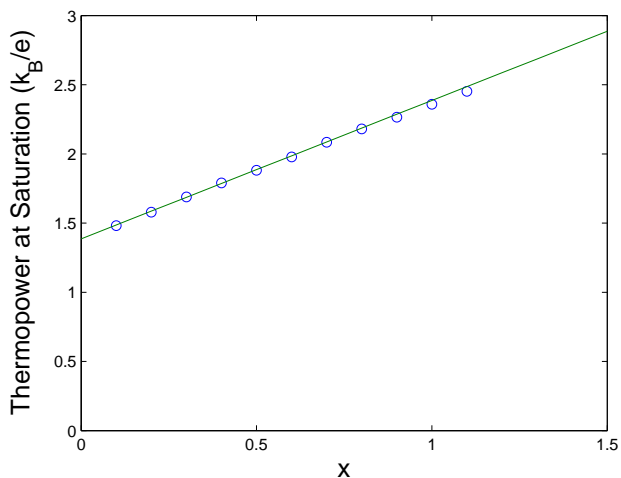


FIG. 4: At high temperatures, the thermopower saturates, at a value dependent on  $x$ . The plot shows the saturation values extracted by evaluating Eq. (26) numerically (see Fig. 2), and a linear dependence corresponding to Eq. (38).

the behavior around the localization transition. An experiment performed on  $In_2O_{3-x}$  (both amorphous and crystalline), approaching the Anderson MIT, shortly after Ref. [11], confirmed qualitatively the main features of Eqs. (28) and (29).<sup>13</sup> Values of  $S$  exceeding  $100 \frac{\mu V}{K}$  were achieved. It should be kept in mind that for a good determination of the critical exponent  $x$ , one needs data at low temperatures and small  $\mu - E_m$ . Data too far from the QPT, which is at both  $T = 0$  and  $\mu - E_m = 0$ , will not be in the critical region and may be sensitive to other effects, as will be discussed later.

It has been customary to use only the low temperature conductivity to determine the critical exponent  $x$ . Using similar  $In_2O_{3-x}$  samples, the conductivity was extrapolated in Ref. [34] to  $T = 0$  and those values were plotted against a control parameter which should be proportional to  $\mu - E_m$  when both are small. A value of  $x = .75 - .8$  was found.

It would be much better to use both the above conductivity values and the slopes of  $S(T)$  near  $T = 0$ , according to Eq. (31). An even better way to do that would be to eliminate the control parameter  $\mu - E_m$  from Eqs. (8) and (28), getting

$$\frac{dS}{dT}_{T \rightarrow 0} \sim [\sigma(T=0)]^{-1/x}, \quad (41)$$

not having to determine the additional parameter  $\mu - E_m$  for each case. The data allowed us to effect this only approximately, see Fig. 5, giving  $x \cong 1 \pm .2$ . However getting near the QPT, this procedure appears to be the one of choice.

Obviously, using the two full functions  $\sigma(\mu - E_m, T)$

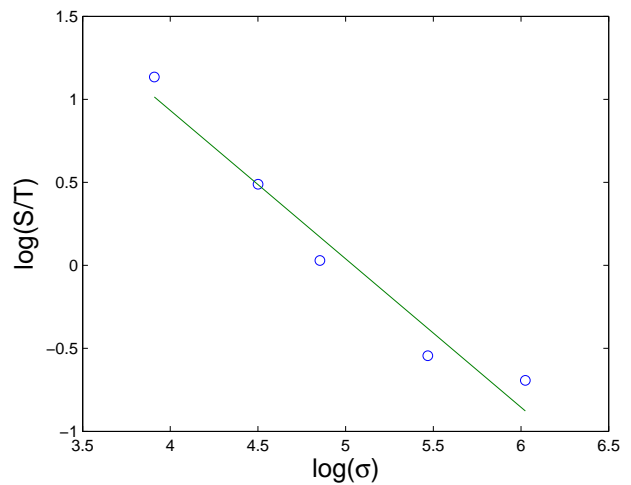


FIG. 5: A small set of data, which should be taken as a preliminary to more extensive studies, was used to find the critical exponent  $x$ . Eqs. (8) and (28) show that the linear (low-temperature) regime of the thermopower has a slope which has an inverse power-law dependence on the distance from the transition. The slope of the log-log plot gives  $x \sim 1.1$ , with a significant error.

and  $S(\mu - E_m, T)$ , in the critical region would place even more strict constraints on  $x$ . Below, we do this for the existing data, to demonstrate the method. Their scaling works well, but the value of  $x$  obtained is not likely to be the real critical value. This is due to a few caveats which will be mentioned.

Fig. 6 compares the above predictions to the experimental data, taking the exponent  $x$  and the values of  $E_m$  as fitting parameters. Fig. 7 shows the approximate data collapse obtained by rescaling the temperature axis of each of the measurements (corresponding to the appropriate value of  $E_m$ ) as in Eq. (27), and the theoretical curve corresponding to  $x = 0.1$ .

The fit is certainly acceptable. However, the value of  $x = .1$  is both in disagreement with the previously determined value and impossible for noninteracting electrons, since there  $x > 2/3$  in three dimensions. Although, as explained at the end of subsection II B, this constraint may not be valid with interactions, we do not take this last value of  $x$  seriously. Since the saturation value was shown to be approximately given by a  $x + C$ , with  $C \sim 1.39$  (see Eq. (38)), a change of the thermopower by tens of percents will cause a large change in the deduced value of  $x$ . These last fits should be regarded only as demonstrating our recommendations for a possible extension of the analysis of future experimental studies.

At higher temperatures, the analysis will be influenced not only by data that are not in the critical region, but two further relevant physical processes may well come in. Obviously, inelastic scattering (by both phonons and other electrons) will be more important. Moreover, for  $T \gtrsim \mu - E_m$ , some of the transport will occur via hopping of holes below the mobility edge. Their thermopower might cancel some of the contribution of electrons above  $\mu$  and thus reduce the thermopower below the values con-

sidered here. This clearly needs further treatment.

At any rate, the interactions appear to be strongly relevant and may give unexpected values for  $x$ . Measurements at lower temperatures and closer to the transition are clearly needed. Checking simultaneously the behavior of both the conductivity and the thermopower is suggested as the method of choice for this problem.

It must be mentioned that similar experiments on granular Al did not show the expected behavior. It should be kept in mind that the resistivities needed to approach the MIT for  $\sim 100\text{\AA}$  grains are larger<sup>21</sup> than the ones for microscopic disorder. Another relevant issue, which we are going to examine in detail in future work, is that while  $E_F$  is in the  $eV$  range, all the energies (without electron-electron interactions) relevant for localization are smaller by several orders of magnitude than for microscopic disorder. Thus, the temperature range for the enhanced thermopower might well be in the sub  $K$  range, which was not addressed in the experiments. The Coulomb blockade may partially alleviate this, but only when it is operative (not in the metallic regime).

The later experiment of Ref. [35], on  $Si:P$  obtained very modest enhancement of  $S$ , but were stated to have been dominated by effective magnetic impurities, which are known to be strongly relevant for the Anderson transition (e.g. eliminating the weak localization contributions). All these issues have to be clarified.

## V. CONCLUDING REMARKS

In this paper we have shown how to include the thermal current in the Thouless scaling picture of conduction in disordered systems. Expressions were given for the

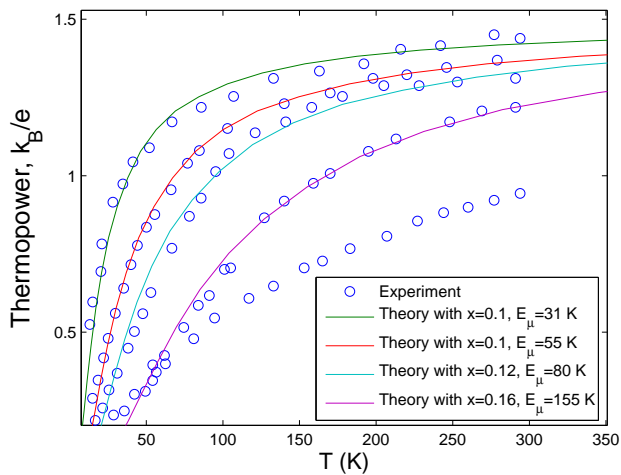


FIG. 6: A fit of the theoretical expression of Eq. (26) to the experimental data. The data was taken from Ref. [13]. The thermopower is measured in units of  $k_B/e \sim 86\mu V/K$ .

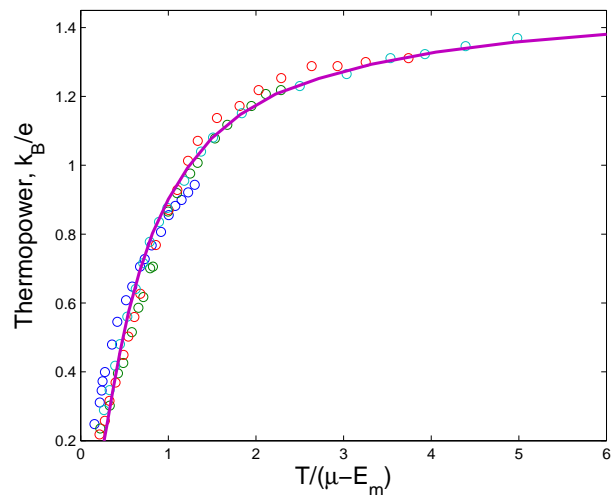


FIG. 7: The 4 data sets of Fig. 6 which are closest to the transition are shown, scaled to lie on a single universal curve, as function of  $T/E_m$ .  $x$  was taken as 0.1 and each curve was given a single value of  $E_m$ .

$2 \times 2$  matrix of longitudinal thermoelectric coefficients, in terms of  $\sigma_0(E)$ , the  $T = 0$  conductivity of the system were its Fermi level fixed at the energy  $E$ . The Onsager relations were shown to hold within this formulation. For the usual critical behavior of  $\sigma_0(E)$ , given by Eq. (1), these behaviors were analyzed for an arbitrary ratio of  $T$  to the distance to the mobility edge. They were shown to satisfy scaling relationships which were confirmed numerically along with their limiting behaviors.

It was shown how the conductivity and thermopower data close to the Anderson QPT should be analyzed simultaneously to yield a better estimate of the critical exponent  $x$  than the determination based on  $\sigma(T)$  alone. This was done for the low-temperature limits of existing data<sup>13,34</sup> on the transition in  $In_2O_{3-x}$ , giving already a good ballpark estimate of  $x$ . The data going to higher (probably too high) temperatures do scale and collapse according to Eq. (27), but the resulting values of  $x$  appear to be too small. One may speculate that this is due to interaction effects, but we prefer to postpone this to after having done this analysis with lower temperature data closer to the transition.

Similar experiments on granular Al do not produce a large and interesting thermopower as above. This is certainly a matter for concern. The explanation might well be due to the smaller microscopic conductivity scales ( $\frac{e^2}{hR}$ ,  $R$  being the grain size), or to the different energy scales relevant for these systems.<sup>21</sup> Alternatively, the inelastic scattering, not treated in this paper, may be relevant as well.

The sharp and asymmetric behavior of  $\sigma_0(E)$  near the transition is ideal for getting large thermopowers. The predicted values approach  $\sim 200 \frac{\mu V}{K}$ . While the experimental results<sup>13</sup> on  $In_2O_{3-x}$  are smaller by  $\sim 40\%$ , this is still encouraging. Were it possible to increase these values say by phonon drag effects, this might even become applicable. Clearly, a treatment of the effects of inelastic scattering on the thermopower is called for, especially including the hopping conductivity regime.

### Appendix A: The heat carried by a transport quasiparticle

To make this analysis useful also for heat transport by phonons, etc., we display the equations for both fermions and bosons. The entropy associated with a state of a given equilibrium system at energy  $E$ , having a population  $f$  is

$$S_E = -k_B [f \ln f + (1 \pm f) \ln(1 \pm f)], \quad (\text{A1})$$

where the upper (lower) sign is for bosons (fermions). When the population  $f$  changes with time, the change of  $S_E$  with time is

$$\dot{S}_E = -k_B \dot{f} \ln \frac{f}{1 \pm f} = -\frac{E}{T} \dot{f}, \quad (\text{A2})$$

where to get the last equality we used the equilibrium  $f = (e^{\frac{E}{T}} \mp 1)^{-1}$ . The outgoing heat current  $T\dot{S}$  is the time derivative of the population times the excitation energy. Thus, each particle leaving the system carries “on its back” an amount of heat  $E$  which is its energy (measured from  $\mu$ ). Summing  $\dot{S}_E$  over all energies shows that the outgoing heat current is given by the outgoing particle current where the contribution of each energy is multiplied by  $E - \mu$ .

It should be noted that the equality of the amounts of  $E - \mu$  and  $-T\dot{S}$  carried by the excitation implies that the relevant free energy does not change when the (quasi)particle moves to another system which is in equilibrium with the first one. This is true for equilibrium fluctuations and also for linear response transport ( $V \rightarrow 0$  and  $\Delta T \rightarrow 0$ ), between the two systems.

As remarked, the result that the heat carried by an electron is given by its energy measured from the chemical potential,  $\mu$ , is valid also for bosons. As a small application, one can easily calculate the net thermal current carried by a single-mode phonon/photon waveguide fed by thermal baths at  $T \pm \Delta T/2$ . The result is a thermal conductance of  $k_B^2 T \pi / (6\hbar)$  (per mode), with no reflections. This agrees with the result of [36]. The sound/light velocity cancels between the excitation velocity and its (1D) DOS, exactly as in the electronic case. This is why this result and the one based on the Wiedemann-Franz law for electrons are of the same order of magnitude. That their numerical factors are equal is just by chance. With reflections due to disorder, once the waveguide’s length is comparable to or larger than the localization length (mean free path for a single mode), its thermal conductance drops markedly.

### Acknowledgments

We thank Uri Sivan, Ora Entin-Wohlman, Amnon Aharony and the late C. Herring for discussions. Special thanks are due to Zvi Ovadyahu for instructive discussions and for making his data available to us. This work was supported by the German Federal Ministry of Education and Research (BMBF) within the framework of the German-Israeli project cooperation (DIP), by the Humboldt Foundation, by the US-Israel Binational Science Foundation (BSF), by the Israel Science Foundation (ISF) and by its Converging Technologies Program. YI is grateful to the Pacific Institute of Theoretical Physics (PITP) for its hospitality when some of this work was done.

- 
- \* Electronic address: Yoseph.Imry@weizmann.ac.il
- <sup>1</sup> P. W. Anderson, Phys. Rev. **109** (1958).
  - <sup>2</sup> N. F. Mott, Adv. Phys. **16**, **49** (1967); Phil. Mag. **17**, 1259 (1968).
  - <sup>3</sup> A. Shalgi and Y. Imry, in E. Akkermans, G. Montambaux, and J. -L. Pichard, eds., *Mesoscopic Quantum Physics*, Les Houches Session LXI, North-Holland, Amsterdam; p. 329. (1995).
  - <sup>4</sup> E. Abrahams, P. W. Anderson, D. C. Licciardello, and T. V. Ramakrishnan, Phys. Rev. Lett. **42**, 673 (1979).
  - <sup>5</sup> A. M. Finkelstein, *Disordered electron liquid with interactions*, this volume; Sov. Phys. J. Exp. Theor. Phys. **57**, 97 (1983); Finkelstein, A. M. Springer Proceedings in Physics, **28**, 230 (1989); For recent references, see also: A. Punnoose and A. M. Finkelstein, Science, **310**, 289 (2005); K. Michaeli and A. M. Finkelstein, Europhys Lett **86**, 27007 (2009).
  - <sup>6</sup> Were one lucky to have very weak interaction in some system, the crossover region to the interaction-dominated behavior would be small and approximate information on the noninteracting critical behavior could be obtained from experiments on this system.
  - <sup>7</sup> B. L. Altshuler and A. G. Aronov, Sov. Phys. **50**, 968 (1980).
  - <sup>8</sup> C. W. J. Beenakker and A. A. M. Staring, Phys. Rev. **B46**, 9667 (1992).
  - <sup>9</sup> A. M. Lunde, K. J. Flensberg and L. I. Glazman, Phys. Rev. Lett., **97**, 256802 (2005).
  - <sup>10</sup> M. Cutler and N. F. Mott, Phys Rev. **181**, 1336 (1969).
  - <sup>11</sup> U. Sivan and Y. Imry, Phys Rev **B 33**, 551 (1986).
  - <sup>12</sup> M. Cutler and J. F. Leavy, Phys. Rev. **133**, A1153 (1964).
  - <sup>13</sup> Z. Ovadyahu, J. Phys. C: Solid State Phys. **19**, 5187 (1986).
  - <sup>14</sup> T. C. Harman and J. M. Honig. *Thermoelectric and Thermomagnetic Effects and Applications*, McGraw-Hill, New York (1967).
  - <sup>15</sup> J. Bardeen, Phys. Rev. Lett. **6**, 57 (1961).
  - <sup>16</sup> W. A. Harrison, *Solid State Theory*, McGraw Hill, New York (1970).
  - <sup>17</sup> D. J. Thouless, Phys. Rev. Lett. **39**, 1167 (1977).
  - <sup>18</sup> This symmetry is valid also when there is no symmetry between the blocks (say, when  $N_l(E) \neq N_r(E)$ ). We shall however mainly consider here the case where the blocks are of the same size ( $N_l(E) = N_r(E)$ ), but they usually do have different defect configurations.
  - <sup>19</sup> G. Czycholl, and B. Kramer, Solid State Commun. **32**, 945 (1979).
  - <sup>20</sup> D. J. Thouless, and S. Kirkpatrick, J. Phys. C. **14**, 235 (1981).
  - <sup>21</sup> Y. Imry, *Introduction to mesoscopic physics*, 2nd edition, Oxford, (2002).
  - <sup>22</sup> A. Amir, Y. Oreg and Y. Imry, Phys. Rev. **A 77**, 050101 (2008).
  - <sup>23</sup> J. T. Edwards, and D. J. Thouless, J. Phys. **C5**, 807 (1972).
  - <sup>24</sup> B. Kramer, A. MacKinnon, T. Ohtsuki, and K. Slevin, *Finite-size scaling analysis of the Anderson transition*, this volume.
  - <sup>25</sup> D. S. Fisher, and P. A. Lee, Phys. Rev. B. **23**, 6851 (1981).
  - <sup>26</sup> A. B. Harris, J. Phys. C: Solid State Phys. **7**, 1671 (1974).
  - <sup>27</sup> N. F. Mott, Phil Mag. **13**, 989 (1966); N. F. Mott, Phil. Mag. **19**, 835 (1969); N. F. Mott, Phil. Mag. **22**, 7 (1970).
  - <sup>28</sup> This is because this inequality assures that the characteristic length,  $\xi$ , grows quickly enough near the transition to average out the disorder fluctuations between different volumes of  $\xi^d$ . This implies that no intrinsic inhomogeneity is generated when the transition is approached.
  - <sup>29</sup> H. B. Callen, *An Introduction to Thermodynamics and thermo-statistics*, Wiley, New York (1985);
  - <sup>30</sup> J. M. Ziman *Principles of the Theory of Solids*, Cambridge, (1969).
  - <sup>31</sup> L. Onsager, Phys. Rev. **38**, 2265 (1931).
  - <sup>32</sup> L. D. Landau and E. M. Lifshitz, *Statistical Physics*, Part 1 Pergamon, Oxford (1980).
  - <sup>33</sup> J. E. Enderby and A.C. Barnes, Phys Rev. B. **49**, 5062 (1994).
  - <sup>34</sup> E. Tousson and Z. Ovadyahu, Phys. Rev. **B38**, 12290 (1988).
  - <sup>35</sup> M. Lakner and H. v. Löhneysen, Phys. Rev. Lett. **70**, 3475 (1993).
  - <sup>36</sup> L. G. C. Rego and G. Kirczenow, Phys. Rev. Lett. **81**, 232 (1998).